Journal of ELECTRICAL ENGINEERING, VOL. 59, NO. 3, 2008, 113–121

HYBRID CONTROL WITH SLIDING–MODE PLUS SELF–TUNING PI FOR ELECTRICAL MACHINES

Ziqian Liu * — **Qunjing Wang** **

This paper presents an approach toward the design of a hybrid speed control with sliding-mode plus self-tuning PI for induction motors. As the variations of both control system parameters and operating conditions occur, the conventional control methods may not be satisfied further. Sliding-mode control is robust with respect to both induction motor parameter variations and external disturbances. By embedding a self-tuning PI control into the sliding-mode control, the chattering problem, which is the main disadvantage in sliding-mode control, can be suppressed. Meanwhile, PI parameters are derived by applying the method of gradient descent optimization to the parameter space to achieve self-tuning online. This makes the PI control robust to changes in the induction motor drive. In addition, a low-pass filter is put after speed controller to smooth discontinuous control signal in order to achieve a smooth torque control. Simulation results show that good transient and steady state responses can be obtained by applying the proposed control, *ie*, the system achieves fast response, overshoot suppression, zero steady-state error, and strong robustness.

K e y w o r d s: sliding-mode control, self-tuning PI control, gradient descent optimization, hybrid speed control, indirect vector control, induction motor

1 INTRODUCTION

The squirrel-cage induction motor is the prime choice of variable-speed drivers in a wide field of applications due to their low cost, simple and rugged construction, high reliability, and minor maintenance. However, because of its highly coupled nonlinear structure and its parameters, which vary with temperature, frequency and current amplitude, it is necessary to develop advanced control techniques in order to improve the control performance.

The vector control of induction motor drives for general industry applications and production automation has been used commonly. However, its decoupling characteristics are highly sensitive to many factors such as the motor magnetic saturation, the alteration of the motor winding temperature or the variation of the motor internal parameters. These factors can break the decoupling condition and cause poor performance of the control system, [1] and [2]. Therefore, many researchers have made great efforts to explore advanced control techniques for the speed control of induction motor drives. For example, the optimal control in [3], adaptive control in [4], robust control in [5], variable-structure system (VSS) control in [6] and intelligent control in [7] and [8] are presented.

It is well known that the sliding-mode controller is one of the most effective methods in reducing the performance degradation due to large system parameter changes and disturbances. In general, it has the following features: high accuracy, fast dynamic response, maintaining stability, simplicity in design and implementation, and robustness. Robustness or low sensitivity to deviations of system parameters and external disturbances is a very important design index of the controller in industrial applications. However in practical applications, a pure sliding-mode control suffers the chattering problem. The chattering occurs mainly because the switching cannot be achieved instantaneously. In order to reduce or overcome that problem, some authors proposed several methodologies to deal with it in [1] and [2]. Here in our work we apply self-tuning PI control plus sliding-mode control into a hybrid controller to suppress the chattering and to get good performances for control system. Because of the variation and high uncertainty of the induction motor internal parameters, it is difficult to tune the PI control gains if we use the conventional PI control. Recently some papers talked about this problem [9]. In this paper, we use a self-tuning PI control which is derived by using the method of gradient descent optimization to the parameter space [19]. Consequently the PI control gains are adjusted automatically online. We do not need to get knowledge of the induction motor to be controlled. Therefore this makes our controller robust to changes of the induction motor parameters. The theoretical derivation, modeling work, and simulation results will be illustrated in following sections. The remainder of this paper is organized as follows. First, a brief review of the induction motor modeling under the indirect vector current control is given. Next, we present the design principles of hybrid speed control and the corresponding algorithms. Then the simulation results and discussions are given. Finally, this paper ends with the conclusion.

2 PRINCIPLE OF INDUCTION MOTOR MODELING WITH INDIRECT VECTOR CONTROL

Given several assumptions [10], the dynamical model of an induction motor in a fixed reference frame attached

* SUNY Maritime College, USA; zliu@sunymaritime.edu ** Anhui University of Technology, China

ISSN 1335-3632

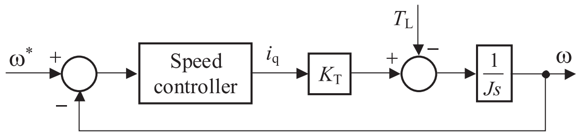

Fig. 1. Speed control design for induction motor with rotor-flux-oriented vector control

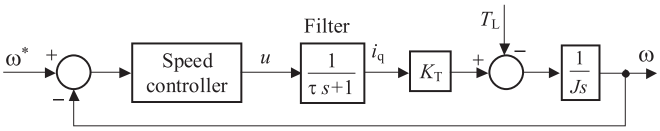

Fig. 2. Block diagram of speed control design after putting a filter

to the stator can be described as follows:

$$\frac{\mathrm{d}\omega}{\mathrm{d}t} = \frac{M}{JL_r}(\psi_a i_b - \psi_b i_a) - \frac{T_L}{J}, \tag{1}$$

$$\frac{\mathrm{d}\psi_a}{\mathrm{d}t} = -\frac{R_r}{L_r}\psi_a - \omega\psi_b + \frac{R_r}{L_r}M i_a, \tag{2}$$

$$\frac{\mathrm{d}\psi_b}{\mathrm{d}t} = -\frac{R_r}{L_r}\psi_b + \omega\psi_a + \frac{R_r}{L_r}M i_b, \tag{3}$$

$$\frac{\mathrm{d}i_a}{\mathrm{d}t} = \frac{MR_r}{(L_rL_s - M^2)L_r}\psi_a + \frac{M}{L_rL_s - M^2}\omega\psi_b - \frac{M^2R_r + L_r^2R_s}{(L_rL_s - M^2)L_r}i_a + \frac{L_r}{L_rL_s - M^2}u_a, \tag{4}$$

$$\frac{\mathrm{d}i_b}{\mathrm{d}t} = \frac{MR_r}{(L_rL_s - M^2)L_r}\psi_b - \frac{M}{L_rL_s - M^2}\omega\psi_a - \frac{M^2R_r + L_r^2R_s}{(L_rL_s - M^2)L_r}i_b + \frac{L_r}{L_rL_s - M^2}u_b \tag{5}$$

where: rotor speed ω, rotor fluxes (ψ_a, ψ_b), and stator currents (i_a, i_b) are state variables. rotor inertia J, stator and rotor inductances (L_s, L_r), mutual inductance M, stator and rotor resistances (R_s, R_r) are system parameters. Control inputs are stator voltages (u_a, u_b).

For the purpose of current control of induction motor using rotor-flux-oriented vector technique, the model of induction motor can be represented on d-q rotating axis, where the d-axis is aligned with the rotor flux at all time and the q-axis is always 90° ahead of the d-axis. Therefore, we take new variables similar to [11] as follows:

$$\begin{bmatrix}\psi_d\\ \psi_q\end{bmatrix} = \begin{bmatrix}\cos\varphi & \sin\varphi\\ -\sin\varphi & \cos\varphi\end{bmatrix}\begin{bmatrix}\psi_a\\ \psi_b\end{bmatrix}, \tag{6}$$

$$\begin{bmatrix}i_d\\ i_q\end{bmatrix} = \begin{bmatrix}\cos\varphi & \sin\varphi\\ -\sin\varphi & \cos\varphi\end{bmatrix}\begin{bmatrix}i_a\\ i_b\end{bmatrix}, \tag{7}$$

$$\begin{bmatrix}u_d\\ u_q\end{bmatrix} = \begin{bmatrix}\cos\varphi & \sin\varphi\\ -\sin\varphi & \cos\varphi\end{bmatrix}\begin{bmatrix}u_a\\ u_b\end{bmatrix}. \tag{8}$$

Variables on left side represent the components of rotor fluxes, stator currents and stator voltage vectors, respectively, with respect to the d-q rotating axis at speed ω_e and identified by the angle φ. In the new state coordinates $(\omega, \psi_d, \psi_q, i_d, i_q)$ and new control coordinates (u_d, u_q), the motor dynamics become:

$$\frac{\mathrm{d}\omega}{\mathrm{d}t} = \frac{M}{JL_r}(\psi_d i_q - \psi_q i_d) - \frac{T_L}{J}, \tag{9}$$

$$\frac{\mathrm{d}\psi_d}{\mathrm{d}t} = \frac{R_rM}{L_r}i_d - \frac{R_r}{L_r}\psi_d + (\omega_e - \omega)\psi_q, \tag{10}$$

$$\frac{\mathrm{d}\psi_q}{\mathrm{d}t} = \frac{R_rM}{L_r}i_q - \frac{R_r}{L_r}\psi_q - (\omega_e - \omega)\psi_d, \tag{11}$$

$$\frac{\mathrm{d}i_d}{\mathrm{d}t} = -\Big(\frac{L_rR_s}{L_rL_s - M^2} + \frac{M^2R_r}{(L_rL_s - M^2)L_r}\Big)i_d + \omega_e i_q + \frac{MR_r}{(L_rL_s - M^2)L_r}\psi_d + \frac{M}{L_rL_s - M^2}\omega\psi_q + \frac{L_r}{L_rL_s - M^2}u_d, \tag{12}$$

$$\frac{\mathrm{d}i_q}{\mathrm{d}t} = -\Big(\frac{L_rR_s}{L_rL_s - M^2} + \frac{M^2R_r}{(L_rL_s - M^2)L_r}\Big)i_q - \omega_e i_d + \frac{MR_r}{(L_rL_s - M^2)L_r}\psi_q + \frac{M}{L_rL_s - M^2}\omega\psi_d + \frac{L_r}{L_rL_s - M^2}u_q. \tag{13}$$

When the current-controlled PWM inverter is applied, the model can be reduced to a third-order system, which is widely used in the induction motor control design ([13], [14], and [15]).

$$\frac{\mathrm{d}\omega}{\mathrm{d}t} = \frac{M}{JL_r}(\psi_d i_q - \psi_q i_d) - \frac{T_L}{J}, \tag{14}$$

$$\frac{\mathrm{d}\psi_d}{\mathrm{d}t} = \frac{R_rM}{L_r}i_d - \frac{R_r}{L_r}\psi_d + (\omega_e - \omega)\psi_q, \tag{15}$$

$$\frac{\mathrm{d}\psi_q}{\mathrm{d}t} = \frac{R_rM}{L_r}i_q - \frac{R_r}{L_r}\psi_q - (\omega_e - \omega)\psi_d. \tag{16}$$

According to the rotor-flux-oriented vector control [16], the rotor flux is aligned with the d axis and kept at a constant so that we have the following relations in steady state [19]:

$$\psi_q = \dot{\psi}_q = 0, \tag{17}$$

$$\psi_d = \psi_r = \text{const.} \tag{18}$$

Applying (17) and (18) into (15) and (16), we can get the slip frequency and the flux current in steady state:

$$\omega_s = \omega_e - \omega = \frac{R_rM}{L_r\psi^*}i_q = \frac{M}{T_r\psi^*}i_q, \tag{19}$$

$$i_d = \frac{\psi^*}{M}. \tag{20}$$

The vector control technique shown above, guarantees that the transient terms vanish in short time. Therefore the steady state equations are sufficient for the derivation of speed control design. The control objective now

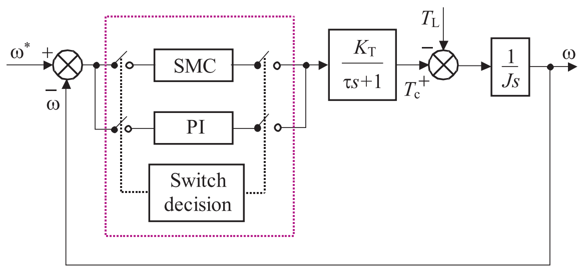

Fig. 3. Hybrid speed controller design diagram

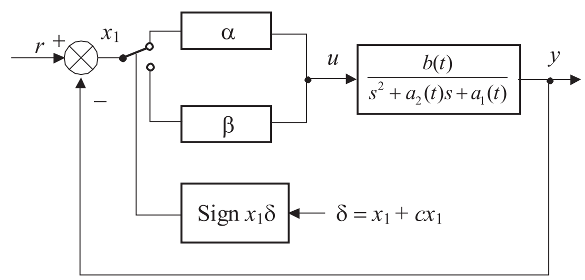

Fig. 4. Sliding-mode control for the second-order system

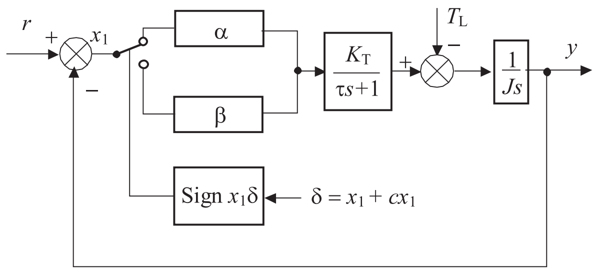

Fig. 5. The design of Sliding-mode control for induction motor

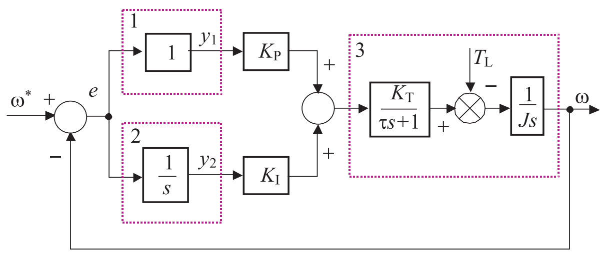

Fig. 6. The design of self-tuning PI for induction motor

is to design a speed controller so that ω tracks ω^*. As a consequence, Fig. 1, in which $K_T = \frac{M\psi^*}{L_r}$, shows the block diagram of speed control design. Compared with the existing results on sliding-mode control of induction motor ([17], [18]), we hope that our control strategy will alleviate the bang-bang switching effect which may excite the mechanical resonance and cause excessive mechanical wearing. Because sliding-mode control belongs to the relay type, this disadvantage mentioned above is normal [18]. In order to achieve a smooth torque control, we put a first-order low-pass filter into our control system. See Fig. 2 where the filter is in the control channel:

$$\tau \frac{\mathrm{d}i_q}{\mathrm{d}t} + i_q = u \,. \tag{21}$$

In this equation, u which is the input of the filter, can be considered as a torque control signal and τ is a time constant. By doing so, the discontinuous control signal passing through the filter gives rise to a continuous control signal.

3 DESIGN PRINCIPLES OF HYBRID SPEED CONTROLLER

Among all existing speed control methods, the most common and widely used one is the PI control. However, it is very difficult to get the good transient performance when the system is subject to uncertainties if we only use PI control as speed controller. Sliding-Mode Control is a promising control technique that can offer good control performance, such as the external disturbances rejection and insensitivity to parameters variations. But it suffers the chattering problem.

We construct a speed controller that combines both together with a suitable switch decision to overcome both disadvantages.

Since our design is based on the induction motor indirect rotor-flux-oriented vector control with the fast current-controlled PWM inverter and the speed controller takes Sliding-Mode Control plus self-tuning PI control into a hybrid controller to suppress the chattering and get good performances for control system. Therefore, the control design diagram can be illustrated as Fig. 3.

A. Sliding-Mode Control Design

Let us consider a second-order system with uncertain parameters:

$$\frac{\mathrm{d}x_1}{\mathrm{d}t} = x_2 \,, \tag{22}$$

$$\frac{\mathrm{d}x_2}{\mathrm{d}t} = -a_2(t)x_2 - a_1(t)x_1 - b(t)u \tag{23}$$

$$\text{where} \quad a_{1\,\min} \le a_1(t) \le a_{1\,\max}$$

$$a_{2\,\min} \le a_2(t) \le a_{2\,\max} \,, b_{\min} \le b(t) \le b_{\max} \,,$$

and $a_1(t)$, $a_2(t)$, $b(t)$ are piecewise-continuous. For the system represented by (22) and (23) above, we hope to design a state variable feedback controller, which is a function of the state variable x_1, that is,

$$u = \phi x_1 \,. \tag{24}$$

According to the principles of sliding-mode control, ϕ can be chosen as

$$\phi = \begin{cases} \alpha \,, & x_1\delta > 0 \,, \\ \beta \,, & x_1\delta < 0 \end{cases} \tag{25}$$

where $\delta = x_2 + cx_1 = 0$ is the switching line. In the equation (25), α and β can be obtained as the following

$$\alpha \geq \max \frac{1}{b(t)} \left[ca_2(t) - c^2 - a_1(t)\right] \quad \text{for } \{a_1, a_2, b\},$$

$$\beta \leq \min \frac{1}{b(t)} \left[ca_2(t) - c^2 - a_1(t)\right] \quad \text{for } \{a_1, a_2, b\}.$$

Therefore, the equivalent block diagram corresponding to the second-order sliding-mode control system above can be shown as Fig. 4. In this paper, if we apply the sliding-mode control to the speed control of induction motor described by Fig. 3, the control system can be represented by a second-order primary feedback sliding-mode control system, which can be described as Fig. 5.

B. Self-Tuning PI Control Design

The most popular speed control used in conventional motor control is PI control because the PI control is simple and reliable to implement. However, since the variation and high uncertainty of the induction motor internal parameters, the tuning of PI control gains becomes a challenging problem. In this study, we use the concept of gradient descent optimization to develop a self-tuning PI control and eliminate any dependence on the control model of induction motor. First, we partition the whole system into three parts as shown in Fig. 6, which is similar to the one given in [12]. Part 1 is the proportional part with exception of proportional gain K_p. Part 2 is the integral part with exception of integral gain K_I. Part 3 is the control plant. Then we consider K_P and K_I as independent variables. Based on the principle of gradient descent optimization, we define an objective function as:

$$E = \frac{1}{2}e^2 = \frac{1}{2}(\omega^* - \omega)^2 . \tag{26}$$

Using the algorithm of gradient descent:

$$\dot{K} - = \eta \frac{\mathrm{d}E}{\mathrm{d}K}, \quad K = \{K_p, K_I\} \tag{27}$$

and following the derivation of paper [19], we can obtain the following tuning algorithm:

$$\dot{K}_p = \eta e y_1 , \quad \dot{K}_I = \eta e y_2 \tag{28}$$

where η is an adaptive coefficient.

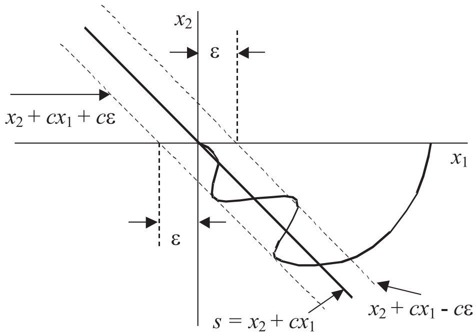

Fig. 7. The diagram of hybrid controller design

The control objective of our tuning algorithms is to bring the motor speed ω to a desired speed command ω^*. This is given in the following theorem.

THEOREM 1. *For any speed control of indirect vector control of induction motor drive, if PI control gains are adapted according to* (28) *with an objective function as* (26)*, then the control achieves global asymptotic speed tracking, ie*

$$\lim_{t\to\infty} (\omega^* - \omega) = 0 . \tag{29}$$

Proof. The proof of this theorem is greatly simplified by using the concept of Lyapunov stability. The objective function defined for the system is written as:

$$E = \frac{1}{2}e^2 . \tag{30}$$

Take its derivative in terms of K which is the space of controller's parameters:

$$\frac{\mathrm{d}E}{\mathrm{d}K} = e\frac{\mathrm{d}e}{\mathrm{d}K} . \tag{31}$$

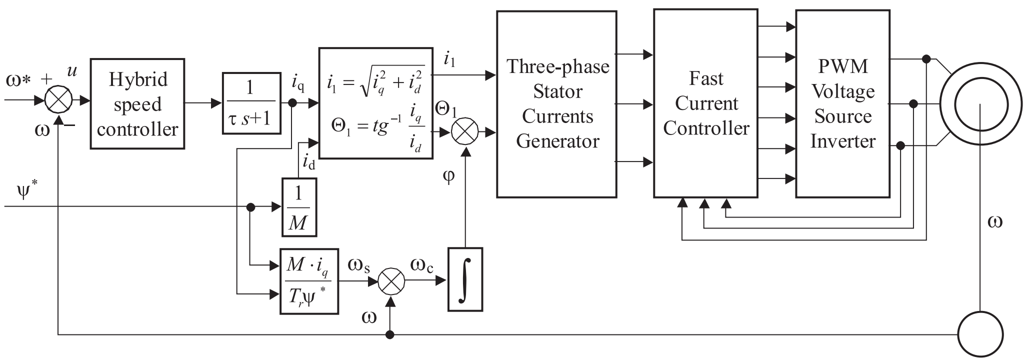

Fig. 8. The whole block diagram of the induction motor drive system

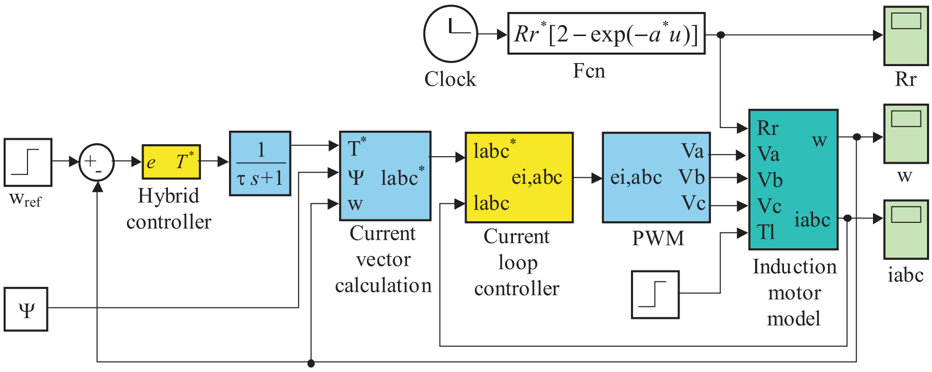

Fig. 9. Matlab/Simulink model of the induction motor drive system

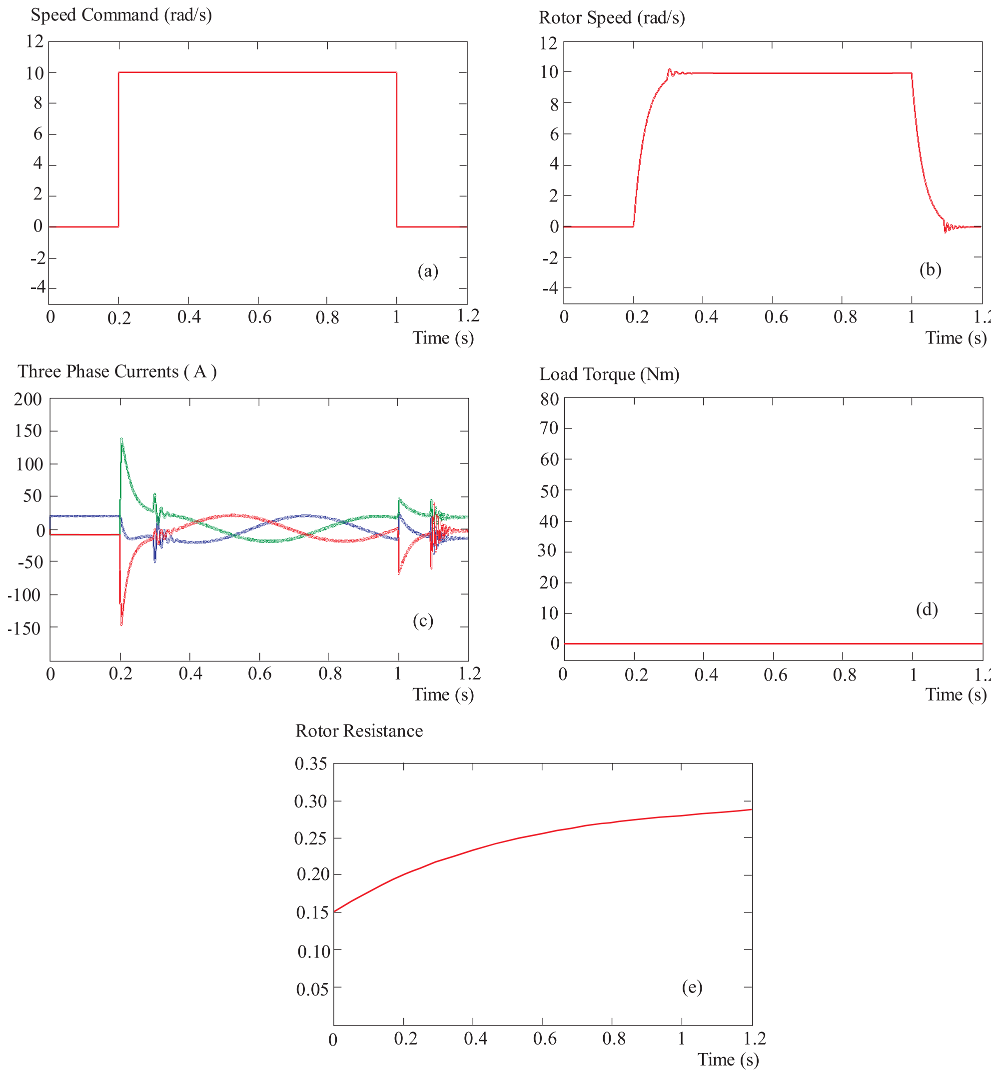

Fig. 10. Dynamic behaviors of induction motor without load: (a)– Speed command,(b) – Rotor speed, (c)– Three-phase currents, (d)– Load torque, (e) – Rotor resistance

Let us choose the E as the Lyapunov function:

$$E = \frac{1}{2}e^2 \geq 0\,, \tag{32}$$

the time derivative $\dot{E}$ is

$$\dot{E} = e\frac{\mathrm{d}e}{\mathrm{d}K}\dot{K}\,. \tag{33}$$

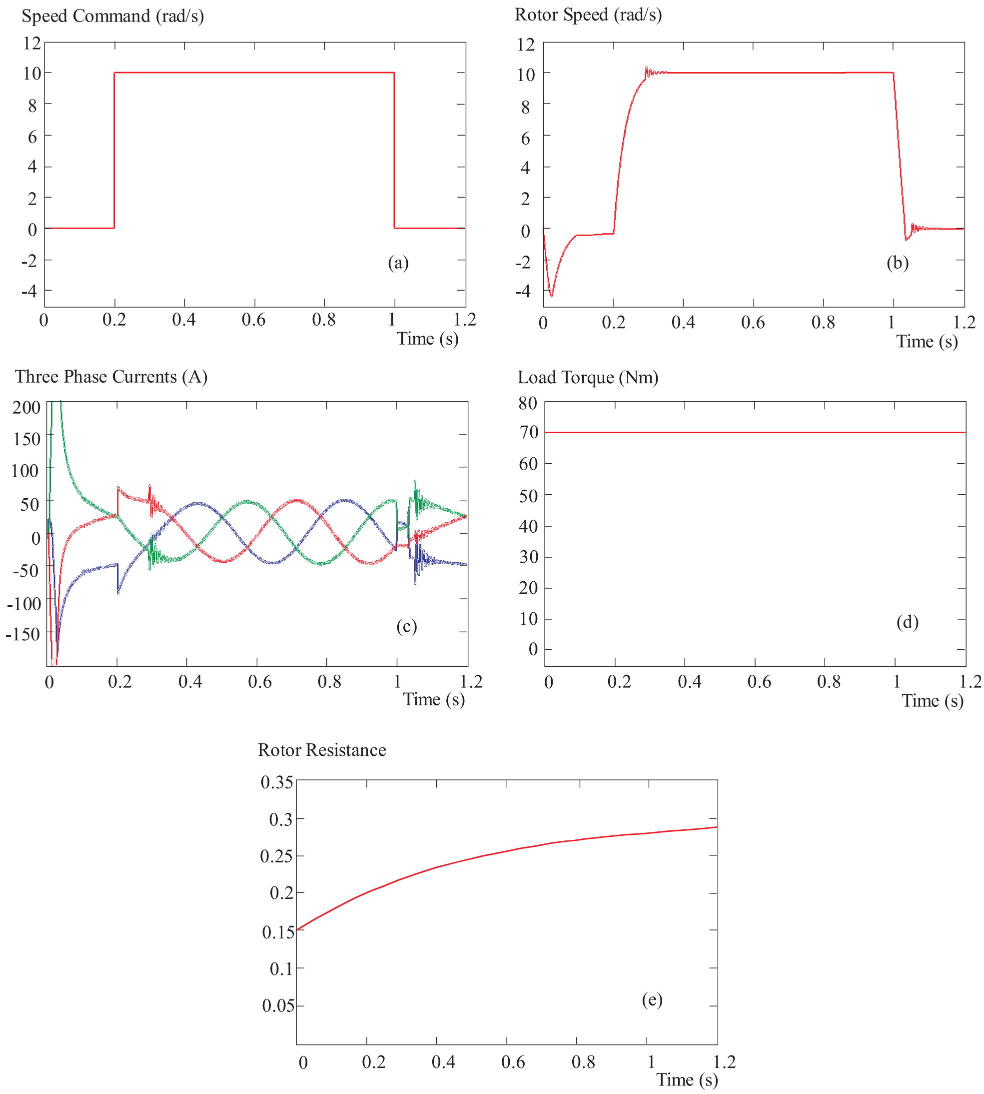

Fig. 11. Dynamic behavior of induction motor with load: (a) – Speed command,(b)– Rotor speed, (c) – Three-phase currents, (d) – Load torque, (e)– Rotor resistance

Considering equation (27), we have

$$\dot{E} = e\frac{\mathrm{d}e}{\mathrm{d}K}\Big(-\eta\frac{\mathrm{d}E}{\mathrm{d}K}\Big) = e\frac{\mathrm{d}e}{\mathrm{d}K}\Big(-\eta e\frac{\mathrm{d}e}{\mathrm{d}K}\Big) = -\eta^2\Big(\frac{\mathrm{d}e}{\mathrm{d}K}\Big)^2 \le 0\,. \qquad (34)$$

From the equation above, we know that E will decrease monotonically with time. Therefore, it can be concluded that

$$\lim_{t\to\infty}(\omega^* - \omega) = 0\,.$$

C. Hybrid Controller Design

The proposed controller combines the sliding-mode control and self-tuning PI control. The control law switches between the sliding-mode control and PI control. It is important to know the switch conditions between both. The idea is illustrated as follows. When the system states are far from the sliding line, the speed controller is the sliding-mode controller. This sliding-mode controller drives system states to hit the sliding line, even under unknown system uncertainties. When the system states approach the sliding line and hit the boundary layer, the PI controller starts to work and ensures that the system states eventually reach the equilibrium point under the system parametric variations and disturbances, as illustrated in Fig. 7. In which ϵ represents small boundary layer.

4 SIMULATION RESULTS

In order to evaluate and validate the effectiveness of our proposed control design presented in the preceding section, a simulation program has been developed using Matlab/Simulink. Figure 8 shows the block diagram of the induction motor drive system.

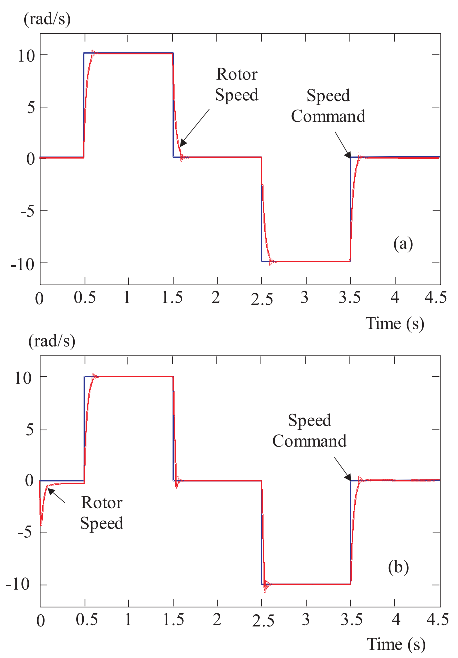

Fig. 12. (a)– Speed response in four quadrants without load, (b)– Speed response in four quadrants with 100% load

In Fig. 8, the outputs of three-phase stator currents generator are

$$i_a^* = |i_1| \sin(\omega_e t + \theta_1)\,,$$
$$i_b^* = |i_1| \sin(\omega_e t + \theta_1 + 120^\circ)\,,$$
$$i_c^* = -(i_a^* + i_b^*)\,.$$

The specifications for the induction motor are: motor power = 15 KW (rated), load torque = 70 NM (rated), rotor flux linkage = 1.3 Wb (rated), angular speed = 220 rad/s (rated), $n = 1$, $J = 0.0586\,\mathrm{kgm}^2$, $R_s = 0.18\,\Omega$, $L_s = 0.0699$ H, $M = 0.068$ H, $R_r = 0.15\,\Omega$, $L_r = 0.0699$ H. In our simulation, we take the change of rotor resistance as $R_s(t) = R_s^*(2 - \exp(-at))$ in which $a = 2$ and give different load torque. The controller parameters are chosen as: $\alpha = 255$, $\beta = 1$, $c = 20$, $\tau = 0.016$, $\eta = -200$, $\varepsilon = 0.5$. In order to evaluate and validate the effectiveness of our proposed control design presented in the previous sections, a simulation program has been developed using Matlab/Simulink. The modules of the simulation program are shown in Fig. 9. Let us look at the transient and steady performances of induction motor after the proposed method is applied for both with a load torque and without load torque. Figure 10 illustrates the dynamic behaviors of induction motor without load torque. Figure 10 (a) displays the signal of command speed. Figure 10 (b) shows the curve of rotor speed. Figure 10 (c) depicts the signals of three-phase stator currents. Figure 10 (d) presents the load torque. Figure 10 (e) is the signal of rotor resistance. Figure 11 indicates the dynamic behaviors of induction motor with 100 % load torque. Figure 11 (a) exhibits the signal of command speed. Figure 11 (b) manifests the curve of rotor speed. Figure 11 (c) points the signals of three-phase stator currents. Figure 11 (d) reveals the load torque and Fig. 11 (e) is the signal of rotor resistance.

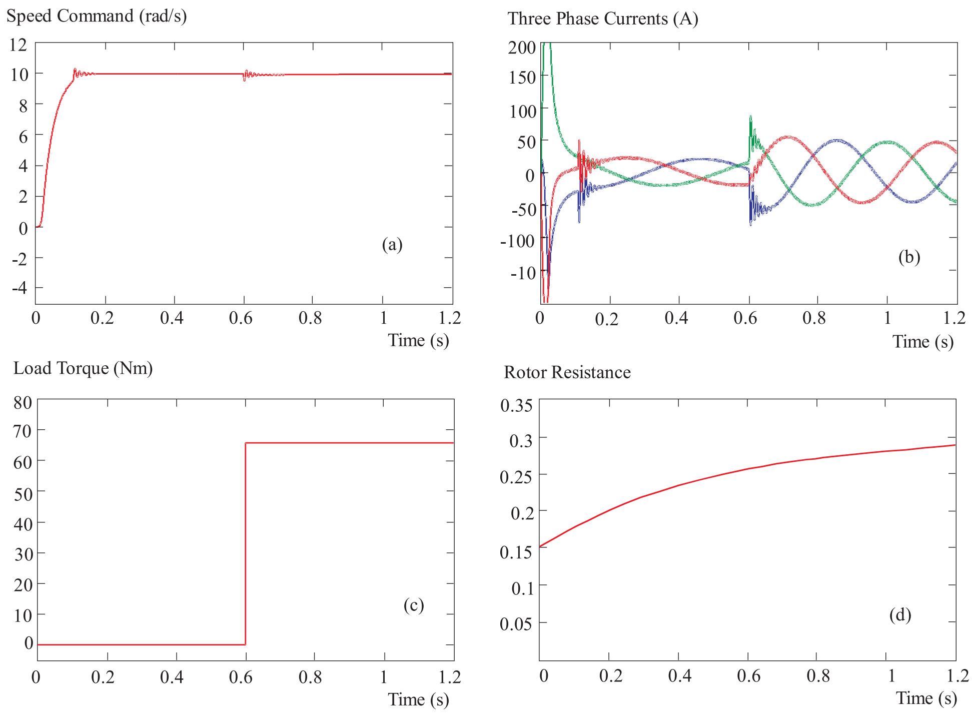

Fig. 13. Dynamic behavior of induction motor with load change from 0 to 100%: (a)– Rotor speed, (b) – Three-phase currents, (c) – Load torque, (d)– Rotor resistance

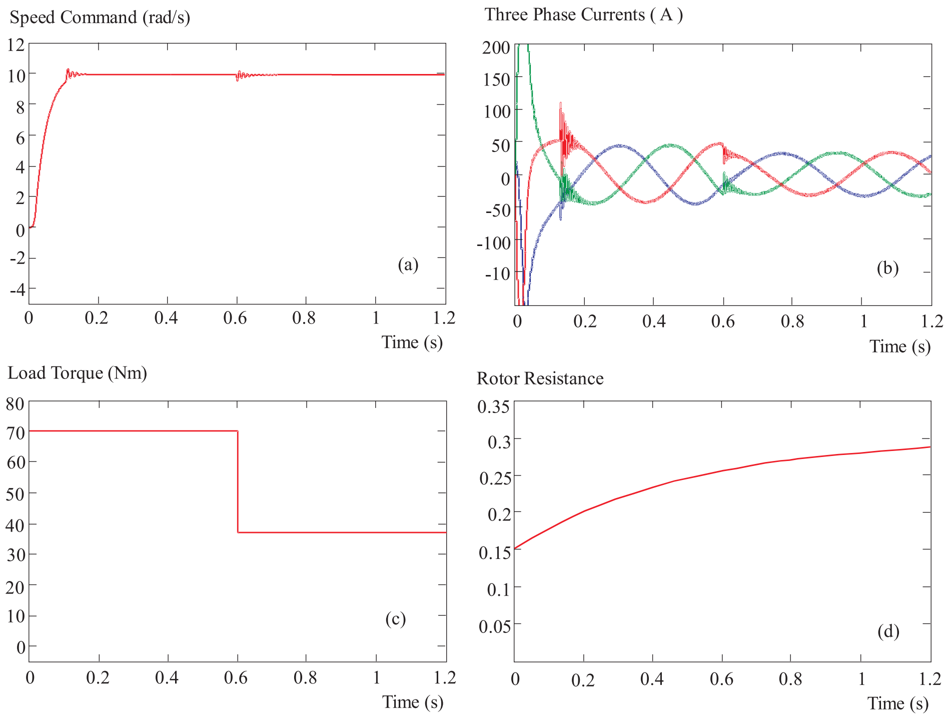

Fig. 14. Dynamic behaviors of induction motor with load change from 100 % to 50 %. (a) Rotor speed. (b) Three-phase currents. (c) Load torque. (d) Rotor resistance.

From Fig. 10 and Fig. 11 one can see the good performances of induction motor when our proposed control was applied. Then let us see the dynamic behaviors of induction motor from Fig. 12 when it runs in four quadrants. In Fig. 12 (a) the motor is running in four quadrants without load. In Fig. 12 (b) the motor is running in four quadrants with 100 % load. From Fig. 12 one can see the performances of induction motor are very well. Moreover, we conduct more tests with the change of load torque to look at the performances of our control method, when the induction motor is running. The first is that the motor starts without load and suddenly is put 100 % load torque at $t = 0.6$ s. This case is presented by Fig. 13. The second is that the motor starts with 100 % load and suddenly the load is reduced to 50 % rated value at $t = 0.6$ s. Figure 14 reveals the results. From Fig. 13 and Fig. 14, the results show that the proposed controller has very good robustness.

5 CONCLUSION

In this paper, a new design approach of hybrid speed control for induction motors has been presented. This controller combines both sliding-mode control and a new self-tuning PI control automatically in order to achieve strong robustness and to suppress the chattering problem. In addition, a low-pass filter is put after speed controller to smooth discontinuous control signal in order to achieve a smooth torque control. The simulation results show that the control system has good dynamic and static performances. The robustness of the controller has also been observed.

References

[1] LIAW, C. M.—LIN, Y. M.—CHAO, K. H.: A VSS Speed Controller with Model Reference Response for Induction Motor Drive, IEEE Trans. Ind. Electron. **48** No. 6 (Dec 2001).

[2] LI, Y. etal: The Self-Adjustable Fuzzy Sliding Mode Control for AC Speed Drive Systems, in 2000 American Control Conference, Chicago, 2000.

[3] KIM, G. T.—KIM, K. S.—PARK, M. H.—WON, C. T.—AHN, D. S.: Time Optimal Control for Induction Motor Servo System, in Proceedings IEEE PESC'88,1988.

[4] LIN, F. J.—LIAW, C. M.: Reference Model Selection and Adaptive Control for Induction Motor Drives, IEEE Trans. Automat. Contr. **38** (Oct 1993), 1594–1600.

[5] LIAW, C. M.—LIN, F. J.: A Robust Speed Controller for Induction Motor Drives, IEEE Trans. Ind. Electron. **41** (June 1994), 308–315.

[6] HUNG, J. Y.—GAO, W. B.—HUNG, J. C.: Variable Structure Control: A Survey, IEEE Trans. Ind. Electron. **40** (Feb 1993), 2–22.

[7] KUNG, Y. S.—LIAW, C. M.: A Fuzzy Controller Improving a Linear Model Following Controller for Motor Drives, IEEE Trans. Fuzzy Syst. **2** (Aug 1994), 194–202.

[8] KUNG, Y. S.—OUYANG, M.—LIAW, C. M.: Adaptive Speed Control for Induction Motor Drives using Neural Networks, IEEE Trans. Ind. Electron. **42** (Feb 1995), 25–32.

[9] CHANG, G. W.—PEREZ, G. E.—MENDES, E.—ORTEGA, R.: Tuning Rules for the PI Gains of Field-Oriented Controllers of Induction Motors, IEEE Trans. Ind. Electron. **47** No. 3 (June 2000).

[10] MARINO, R.—TOMEI, P.: Nonlinear Control Design: Geometric, Adaptive and Robust, Prentice-Hall, London, 1995.

[11] MARINO, R.—PERESADA, S.—TOMEI, P.: Global Adaptive Output Feedback Control of Induction Motors with Uncertain Rotor Resistance, IEEE Trans. Automat. Contr. **44** (May 1999), 967–983.

[12] LIN, F.—BRANDT, R. D.—SAIKALIS, G.: Self-Tuning of PID Controllers by Adaptive Interaction, in 2000 American Control Conference, Chicago, 2000.

[13] SHYU, K.—SHIEH, H. J.: A New Switching Surface Sliding-Mode Speed Control for Induction Motor Drive Systems, IEEE Trans. Power Electron. **11** (July 1996), 660–667.

[14] MARINO, R.—PERESADA, S.—TOMEI, P.: Output Feedback Control of Current-Fed Induction Motors with Unknown Rotor Resistance, IEEE Trans. Contr. Syst. Technol. **4** (July 1996), 336–347.

[15] BODSON, M.—CHIASSON, V.—NOVOTANK, R.: High-Performance Induction Motor Control via Input-Output Linearization, IEEE Contr.Syst. Mag. **14** (Jan 1994), 25–33.

[16] BOSE, B. K.: Power Electronics and AC Drives, Prentice-Hall, Englewood Cliffs, NJ, 1986.

[17] SHYU, K.—SHIEH, H. J.: A New Switching Surface Sliding-Mode Speed Control for Induction Motor Drive Systems, IEEE Trans. Power Electron. **11** (July 1996), 660–667.

[18] HO, Y. Y.—SEN, P. C.: Control Dynamics of Speed Drives Systems using Sliding Mode Controllers with Integral Compensation, IEEE Trans. Ind. Applicat. **27** (Sep/Oct 1991), 883–892.

[19] LIU, Z.: Self-Tuning Control of Electrical Machines Using Gradient Descent Optimization, Optimal Control Applications and Methods **28** (Mar/Apr 2007), 77–93.

Received 13 March 2007

Ziqian Liu (PhD) is currently an Assistant Professor of Electrical Engineering at SUNY Maritime College, Throggs Neck, New York, USA. From 1989 to 1999, he worked with the Department of Electrical Engineering at Hefei University of Technology, China. His research interests include optimal control, robust control, adaptive systems, artificial neural networks, and motor control systems.

Qunjing Wang received the DSc (Eng) from the University of Science & Technology of China (USTC). He has worked for the Department of Electrical Engineering at Hefei University of Technology where he is presently a Professor of Electrical Engineering. Dr Wang is responsible for the research activities at Hefei University of Technology in the area of Electrical Engineering and Power Electronics.